

1 **Projected pH reductions by 2100 might put deep North Atlantic**
2 **biodiversity at risk.**

3 **M. Gehlen¹, R. S  f  rian², D. O. B. Jones³, T. Roy⁴, R. Roth⁵, J. Barry⁶, L. Bopp¹,**
4 **S. C. Doney⁷, J. P. Dunne⁸, C. Heinze^{9,11}, F. Joos⁵, J. C. Orr¹, L. Resplandy¹, J.**
5 **Segschneider¹⁰ and J. Tjiputra¹¹**

6

7 [1] LSCE/IPSL, Laboratoire des Sciences du Climat et de l'Environnement, Orme des
8 Merisiers, CEA/Saclay 91198 Gif-sur-Yvette Cedex, France

9 [2] CNRM-GAME, M  t  o-France-CNRS, Toulouse, France

10 [3] National Oceanography Centre, University of Southampton Waterfront Campus, European
11 Way, Southampton, SO14 3ZH, UK

12 [4] LOCEAN/IPSL, 4, place Jussieu 75252 PARIS Cedex 05, France

13 [5] Climate and Environmental Physics, Physics Institute and Oeschger Centre for Climate
14 Change Research, University of Bern, CH-3012 Bern, Switzerland

15 [6] Monterey Bay Aquarium Research Institute, Moss Landing, CA 95039, USA

16 [7] Marine Chemistry and Geochemistry, Woods Hole Oceanographic Institution, Woods
17 Hole, MA 02543, USA

18 [8] National Oceanic and Atmospheric Administration/Geophysical Fluid Dynamics
19 Laboratory, Princeton, NJ 08540, USA

20 [9] Geophysical Institute, University of Bergen and Bjerknes Centre for Climate Research,
21 5007 Bergen, Norway

22 [10] Max Planck Institute for Meteorology, Bundesstr. 53, 20146 Hamburg, Germany

23 [11] Uni Climate, Uni Research AS and Bjerknes Centre for Climate Research, 5007 Bergen,
24 Norway

25 Correspondence to: Marion Gehlen, LSCE/IPSL, Laboratoire des Sciences du Climat et de
26 l'Environnement, UMR CEA-CNRS-UVSQ, Orme des Merisiers, B  t. 712, CEA/Saclay
27 91198 Gif-sur-Yvette Cedex, France; Tel. + 33 1 69 08 86 72; marion.gehlen@lsce.ipsl.fr

28

29 **Abstract**

30 This study aims to evaluate the potential for impacts of ocean acidification on North Atlantic
31 deep-sea ecosystems in response to IPCC AR5 Representative Concentration Pathways
32 (RCP). Deep-sea biota is likely highly vulnerable to changes in seawater chemistry and
33 sensitive to moderate excursions in pH. Here we show, from seven fully-coupled Earth
34 system models, that for three out of four RCPs over 17% of the seafloor area below 500 m
35 depth in the North Atlantic sector will experience pH reductions exceeding -0.2 units by 2100.
36 Increased stratification in response to climate change partially alleviates the impact of ocean
37 acidification on deep benthic environment. We report on major pH reductions over the deep
38 North Atlantic seafloor (depth > 500 m) and at important deep-sea features, such as
39 seamounts and canyons. By 2100 and under the high CO₂ scenario RCP8.5 pH reductions
40 exceeding -0.2, (respectively -0.3) units are projected in close to 23% (~15%) of North
41 Atlantic deep-sea canyons and ~8% (3%) of seamounts – including seamounts proposed as
42 sites of marine protected areas. The spatial pattern of impacts reflects the depth of the pH
43 perturbation and does not scale linearly with atmospheric CO₂ concentration. Impacts may
44 cause negative changes of the same magnitude or exceeding the current target of 10% of
45 preservation of marine biomes set by the convention on biological diversity implying that
46 ocean acidification may offset benefits from conservation/management strategies relying on
47 the regulation of resource exploitation.

48

49 **Keywords: ocean acidification, climate change, deep-sea ecosystems**

50

51 **1 Introduction**

52 Global ocean anthropogenic carbon inventories suggest that the ocean has taken up $\sim 155 \pm$
53 31 PgC (10^{15} g of carbon) in 2010 (Khaliwala et al. (2013)). This uptake of CO_2 is causing
54 profound changes in seawater chemistry resulting from increased hydrogen ion concentration
55 (decrease in pH, $\text{pH} = -\log_{10}[\text{H}^+]$) referred to as ocean acidification (IPCC, 2011).
56 Experimental and modelling studies provide compelling evidence that ocean acidification will
57 put marine ecosystems at risk (e.g. Orr et al., 2005; Kroeker et al., 2013). However, with the
58 exception of assessments focusing on cold-water coral systems (Barry et al., 2005, 2013;
59 Fleege et al., 2006; Guinotte et al., 2006; Tittensor et al., 2010), quantifications of biological
60 consequences of ocean acidification mostly targeted surface ocean or coastal environments
61 (Kroeker et al., 2010). The aim of this study is to extend our understanding of broad scale
62 impacts of ocean acidification from the existing shallow water studies to focus specifically on
63 deep-sea ecosystems. The deep sea is under increasing anthropogenic pressure as
64 technological advances allow exploitation of formerly inaccessible regions (Clauss and Hoog,
65 2002). While waste disposal, fishing and, in the future, mineral extraction are recognized as
66 dominant human pressures (Ramirez-Llodra et al., 2011), expert assessments urge
67 consideration of climate change and ocean acidification impacts in future ecosystem
68 conservation/management strategies (Taranto et al., 2012; Billé et al., 2013).

69

70 While previous studies quantified changes in carbonate mineral saturation state as a measure
71 for potential detrimental impacts on deep calcifying communities (Guinotte et al., 2005, 2006;
72 Turley et al., 2007; Fautin et al., 2009), this model-based assessment uses pH. The tight
73 control of pH at the cellular scale is an important prerequisite of proper cell functioning and
74 mechanisms of pH control are ubiquitous across many taxa (Seibel and Walsh, 2003 and
75 references therein). Deep-sea organisms might be particularly vulnerable to changes in
76 seawater chemistry, at least in part owing to limitations on rate processes, caused by low
77 temperature (Childress, 1995; Seibel and Walsh, 2001) and possibly food availability
78 (Ramirez Llodra, 2002), as well as the environmental stability of their habitat in the past
79 (Barry et al., 2011; Seibel and Walsh, 2003). A recent review (Somero, 2012) highlights the
80 link between environmental stability and the capacity to acclimate to future changes in
81 environmental variables such as pH. According to this study, environmental stability might
82 impair the potential for acclimation. This stands in sharp contrast to shallow water or inter-

83 tidal organisms, which are adapted to a dynamic environment with large changes in
84 temperature and seawater chemistry (Hofmann et al., 2011; Duarte et al., 2013).

85

86 A model sensitivity study (Gehlen et al., 2008) suggested the potential for large pH reductions
87 (up to -0.6 pH units) in the deep North Atlantic. Regions of large pH reductions coincided
88 with areas of deep-water formation. Deep-water formation drives the rapid propagation of
89 surface-derived changes in carbonate chemistry to depth as underlined by high vertically-
90 integrated water column inventories of anthropogenic carbon (Sabine et al., 2014), as well as
91 and tritium, chlorofluorocarbon distributions (Doney and Jenkins, 1994). Gehlen et al. (2008)
92 used output from a single model and for a scenario following an atmospheric CO_2 increase of
93 1% per year over 140 years starting from an atmospheric CO_2 level of 286 ppm. This rate of
94 increase is about twice as large as the rate typical for a high-end IPCC concentration pathway.
95 The study did not include circulation changes in response to climate change.

96 Here we extend the study by Gehlen et al. (2008) by analysing pH projections from seven
97 Earth system models that contributed to the 5th Coupled Model Intercomparison Project
98 CMIP5 and for four different Representative Concentration Pathways (RCP, Van Vuuren et
99 al., 2011) ranging from a strong emission mitigation scenario (RCP2.6) to the high- CO_2
100 scenario RCP8.5. We assess the magnitude of deep-water pH reductions in the North Atlantic
101 (35°N - 75°N , 90°W - 180°W) over this century in response to atmospheric CO_2 increase and
102 climate change. The North Atlantic is a well-ventilated region of the world ocean and, despite
103 a projected increase in stratification, will remain well-oxygenated in the future (Bopp et al.,
104 2013). The study complements assessments by Bopp et al. (2013) and Mora et al. (2013)
105 which evaluated large-scale average pH reductions in response to the same RCP pathways,
106 but without a detailed discussion of spatial patterns and their link to circulation. We define a
107 critical threshold for pH reductions based on evidence from paleo-oceanographic studies,
108 contemporary observations and model results. Future multi-model projections of pH changes
109 over the seafloor are analysed with reference to this threshold and without discrimination of
110 particular habitats first. Next, model results are put into the perspective of ecosystem
111 conservation by evaluating changes in pH against the distribution of seamounts and deep-sea
112 canyons. These features are known as sites of high-biodiversity deep-sea ecosystems, such as
113 cold-water corals and sponge communities (ICES, 2007; Clark MR et al., 2010; De Leo et al.,
114 2010) and are selected as representative examples of deep sea environments.

115

116 **2 Material and methods**

117 **2.1 Earth system models**

118 Our study draws on results from 2 types of Earth system models: (1) the Bern3D-LPJ carbon-
119 cycle/climate model (Steinacher et al., 2013; Roth and Joos, 2013) and (2) seven fully-
120 coupled three-dimensional atmosphere ocean climate models that participated in the 5th
121 Coupled Model Intercomparison Project (CMIP5, Taylor et al., 2011) and contributed to the
122 5th Assessment Report of the Intergovernmental Panel on Climate Change (IPCC AR5). The
123 Bern3D-LPJ is a model of intermediate complexity featuring a 3D geostrophic-balance ocean
124 and 2D atmospheric energy and moisture-balance model. The cycle of carbon and related
125 tracers is represented including prognostic formulations for marine production, a seafloor
126 sediment, and a dynamic global vegetation model. This model is relatively cost-efficient
127 compared to CMIP5 models. It is used to evaluate the order of magnitude of pH reductions
128 associated with past abrupt climate change by analysing results from freshwater hosing
129 experiments (Bryan 1986; Marchal et al., 1999; Matsumoto and Yokoyama, 2013).

130

131 Concerning the subset of CMIP5 models, we selected models for which 3D pH fields were
132 available and that had been part of a published multi-model evaluation (Bopp et al., 2013).
133 We analyse output for four future atmospheric CO₂ concentration scenarios (RCP), along with
134 the corresponding pre-industrial control simulations, piControl. The nomenclature follows
135 CMIP5 recommendations. Historical simulations cover the period between 1870 and 2005
136 and are followed by climate change scenarios according to RCP8.5, RCP6.0, RCP4.5 and
137 RCP2.6 from 2006 to 2100 (Van Vuuren et al., 2011; Moss et al., 2010). RCP identifiers refer
138 to the additional radiative forcing as target for 2150 AD in the Integrated Assessment Models
139 used to derive the RCP scenarios: RCP2.6, RCP4.5, RCP6.0 and RCP8.5 with corresponding
140 atmospheric CO₂ levels of 421, 538, 670 and 936 ppm. Individual RCPs differ with respect to
141 the temporal evolution of atmospheric CO₂ and range from a stringent emission mitigation
142 RCP2.6 to the high-CO₂ scenario RCP8.5. The complete set of RCPs was not available for all
143 models. Please refer to Table S1 (supporting material) for model name, scenario and
144 references.

145 **2.2 Deep-sea ecosystems**

146 This study uses datasets of seamounts (Yesson et al., 2011) and canyons (Harris and
147 Whiteway, 2011). For seamounts, these data include location, height and surface assuming a
148 conical shape. For canyons, the data consist of a high-resolution vector database of canyon
149 centre lines that was converted into a raster dataset of canyon presence (using ArcGIS v10)
150 for analysis. Data were projected on a 1°x1° regular grid.

151 **2.3 Post-treatment of model output and data**

152 **2.3.1 Post-treatment of CMIP5 model output**

153 Model output is interpolated on a regular grid of 1°x1° resolution. Anomalies are computed as
154 the difference between the decade 2090-2099 and the long-term mean of the pre-industrial
155 state. As the focus of this study is on impacts on benthic communities, we quantify pH
156 changes in the deepest model box over a topography range from 500 m to > 4500 m water
157 depth.

158 **2.3.2 Computation of the area of seamounts for impact assessment**

159 The area of North Atlantic seafloor impacted by ocean acidification is estimated on the basis
160 of individual grid cells for which the reduction in pH exceeded ≥ 0.2 or 0.3 units. The
161 impacted area follows as the integral of the area of these 1°x1° grid cells. The area of
162 seamounts with a pH reduction ≥ 0.2 or 0.3 units is computed based on distribution and height
163 assuming a conical shape (Danovaro et al., 2008, Yesson et al., 2011). The database provides
164 height above seafloor and base area. The area of the seamount (A) is given by:

$$165 \quad A = \pi r^2 \sqrt{r^2 + (h+h')^2} \quad (1)$$

166 where, r is the base radius of the seamount and h+h' is the height. The height impacted by a
167 pH reduction exceeding the threshold (h') is diagnosed from the depth of the pH anomaly
168 corresponding to the threshold. The radius of the seamount at the depth of the anomaly (r') is
169 obtained from the Thales theorem:

$$170 \quad \frac{r'}{r} = \frac{h'}{h} \quad (2)$$

$$171 \quad \text{as: } r' = \frac{h'}{h} r \quad (3)$$

172 The final expression of r' is the positive analytical solution of the fourth-order polynomial

$$173 \quad \frac{A^2}{p^2} = \frac{h^2}{h'^2} r'^2 \left(\frac{h^2}{h'^2} r'^2 + (h+h')^2 \right) \quad (4)$$

$$174 \quad \text{as: } r' = \pm \frac{h'}{h} \left[\frac{1}{2} \left(-1 \pm \sqrt{\frac{4A^2}{p^2 h^2}} \right) \right]^{\frac{1}{2}} \quad (5)$$

175 The impacted area of the seamount (A^*) follows from the depth of pH anomaly as a function
176 of seamount height:

$$177 \quad A^* p \frac{h'}{h} \left[\frac{1}{2} \left(-1 + \sqrt{\frac{4A^2}{p^2 h^2}} \right) \right]^{\frac{1}{2}} \left(h'^2 + \frac{h'^2}{h^2} \left[\frac{1}{2} \left(-1 + \sqrt{\frac{4A^2}{p^2 h^2}} \right) \right] \right) \quad (6)$$

178 where A is the total surface area of the seamount.

179

180 **3 Results and discussion**

181 **3.1 Environmental stability and critical threshold for pH reduction**

182 Considering that environmental stability might impair the potential for acclimation, we
183 assessed pH changes over glacial-interglacial time scales and for past events of rapid climate
184 changes recognized for having driven major reorganizations in North Atlantic circulation and
185 carbonate chemistry.

186 The pH is defined as the negative logarithm of the hydrogen ion concentration ($[H^+]$). From
187 the basic properties of logarithms it follows that the difference in pH equals the logarithm of
188 the ratio of hydrogen ion concentrations. For a given pH change, the change in $[H^+]$, $\Delta[H^+]$, is
189 a linear function of the initial hydrogen ion concentration ($[H^+]_i$) as

190 $\Delta[H^+] = [H^+]_i \left((1/10^{\Delta pH}) - 1 \right)$. Hence, the larger the initial $[H^+]$, the larger the perturbation
191 (Fig. S1). Contrasting shallow and deep environments highlights that absolute changes in $[H^+]$
192 are amplified at depth for any threshold, that is for environments of low natural variability.

193 **3.1.1 Glacial-interglacial time-scales**

194 The paleo-record permits evaluation of environmental variability of the deep-ocean over the
195 past million years. Available evidence indicates a low variability over this time interval

196 (Elderfield et al., 2012; Yu et al., 2010; Yu et al., 2013). Changes in carbonate chemistry were
197 small in the deep-ocean compared to surface layers (Yu et al., 2010). Recent studies re-
198 evaluated deep-water pH changes between glacial to present (Sanyal et al., 1995), arguing that
199 carbonate compensation kept deep-water pH close to constant (Hönisch et al., 2008). We use
200 data available in Yu et al. (2010) (and associated supplementary material) and follow their
201 reasoning to infer DIC changes from $[\text{CO}_3^{2-}]$ and hence alkalinity, to compute associated
202 changes in pH for sediment core BOFS 8K (52.5 N, 22.1 W, 4,045 m). This pH change is
203 computed using CO2sys (<http://cdiac.ornl.gov/oceans/co2rprt.html>) with alkalinity and DIC
204 as input variables, along with temperature, depth, phosphate and silicate as (Yu et al., 2010).
205 We estimate a pH reduction of ~ 0.1 pH units for North Atlantic deep-water over the early
206 deglacial (17,500 to 14,500 years before present).

207 3.1.2 Rapid events associated with fresh-water release: Heinrich and 208 Dansgaard Oeschger events

209 Model experiments yield maximum pH reductions in North Atlantic deep-water below 0.15
210 pH units in response to a shut-down of the North Atlantic Meridional Overturning Circulation
211 (AMOC, Fig. 1). To realize an abrupt shutdown of the AMOC different durations of
212 freshwater perturbations in the North Atlantic on top of a pre-industrial steady state have been
213 tested releasing in total 3×10^{15} m³ freshwater (~ 9 m sea level equivalent). In terms of pH
214 changes in the North Atlantic region, the experiment with a 300 yr lasting freshwater forcing
215 of 0.33 Sv results in the strongest response (Fig. 1(a)). In these experiments, the cause of the
216 pH decrease is not high atmospheric CO₂ (CO₂ only increases a few ppm during the
217 freshwater experiment), but is mainly a result of the decrease in deep ocean ventilation. This
218 leads to the additional accumulation of dissolved inorganic carbon (DIC) by the respiration of
219 organic matter. Although alkalinity is also increased in the deep by the dissolution of
220 carbonate particles settling through the water column, it does not compensate the increase in
221 DIC leading to more acidic waters in the deep. The most extreme negative excursion of the
222 pH averaged over the deep (below 2000 m) Northern Atlantic (45° N – 65° N) occurs ~ 150
223 years after the end of the freshwater forcing with a decrease of ~ 0.13 pH units relative to the
224 unperturbed pre-industrial state (Fig. 1(b)). The pH-decrease does not exceed -0.18 pH units
225 in any of the individual grid boxes. In Figure 1 (c) and (d) the spatial distribution of the pH-
226 reduction averaged over years 400-450 (i.e., during the maximum of the pH decrease) is

227 shown in terms of pH anomalies at the seafloor and in a section through the Atlantic at
228 38.5°W.

229 3.1.3 Critical threshold for pH reductions

230 For the purpose of evaluating the potential for negative impacts on deep-sea benthic
231 environments, a critical threshold for pH reduction needs to be identified. Reductions of pH
232 exceeding the envelope set by past and present natural variability are considered as critical.
233 Paleo-evidence suggests that the deep-sea fauna has evolved under conditions of
234 environmental variability confined to a narrow range over the past million years (Yu et al.,
235 2010; Elderfield et al., 2012). Many past episodes of climate change occurred over
236 significantly longer time-scales than the current anthropogenic perturbation of the climate
237 system, allowing carbonate compensation to keep deep-water pH close to constant (Hönisch
238 et al., 2008). This is corroborated by computing pH reduction over glacial-interglacial cycles
239 for a North Atlantic site. Decadal-to-centennial changes are addressed by fresh-water hosing
240 model experiments to simulate effects of circulation changes associated with rapid Heinrich
241 and Dansgaard Oeschger events. In both cases, pH reductions are below 0.15 pH units.
242 Similarly, small amplitude natural temporal pH variability at depth emerges
243 from a multi-annual time series stations (González-Dávila et al., 2010) and the analysis of the
244 long pre-industrial simulation “piControl” (Fig. S2 in the Supplement). In summary, natural
245 pH variations on multi-annual, decadal-to-century, and longer time scales were likely smaller
246 than 0.2 pH units on the regional-to-basin scale in the deep Atlantic and at least for the past
247 million years. This suggests that pH variations of up to 0.1 to 0.2 pH units do not present a
248 risk for marine life.

249

250 This leads us to define two thresholds for pH reduction between pre-industrial and the end of
251 the 21st century: -0.2 and -0.3 pH units. Both stand for pH reductions exceeding paleo-record-
252 based estimates of changes in North Atlantic deep-water chemistry over the past ten-thousand
253 years, as well as being much larger than the amplitude of natural temporal variability of pH in
254 the deep North Atlantic (González-Dávila et al., 2010). The first threshold (-0.2) is in line
255 with recommendations by environmental agencies (Schubert et al., 2006) following the
256 precautionary principle, and is reported to increase mortality of deep-sea benthic organisms
257 during in-situ exposure experiments (Barry et al., 2005). The second threshold (-0.3) allows to

258 bracket a range of changes spanning from a ~58% increase in hydrogen ion concentration up
259 to ~100%.

260

261 **3.2 Projections of pH reductions over the 21st century**

262 Time-series of atmospheric CO₂ (ppm) for three out of four IPCC RCP scenarios between
263 2006 and 2100 show an increase in CO₂ over this century, only RCP2.6 does not show a
264 general increase with time (Fig. 2 (a)). The corresponding simulated pH reductions for surface
265 and deep North Atlantic waters are presented on Fig. 2(a), respectively Fig. 2 (c). Projected
266 pH changes are indicated as multi-model mean along with the between-model spread.
267 Monitoring at time series stations reveals that the observed surface ocean pH decreases tracks
268 increasing atmospheric pCO₂ (Orr, 2011). This trend is confirmed by the decline in simulated
269 surface ocean pH (Fig. 2(b)) with a small between-model spread. In the surface ocean the
270 extent of ocean acidification is set by the atmospheric CO₂ trajectory, along with physical
271 climate change, namely warming and associated changes in ocean circulation and CO₂
272 thermodynamic properties. Surface waters, with high levels of dissolved anthropogenic CO₂
273 and characterised by low pH values, are entrained to the interior ocean during seasonal mixed
274 layer deepening and deep convection episodes. As a result, deep pH changes (Fig. 2 (c))
275 reflect atmospheric CO₂ to a lesser extent. Because the deep water formation differs between
276 models, the inter-model spread is significantly larger in deep waters than for the surface
277 ocean.

278

279 The spatial pattern of pH reductions is exemplified for RCP4.5 and RCP8.5 in Figure 3 (see
280 supplementary material, Fig. S3, for RCP2.6 and RCP6.0). Under RCP4.5 (Fig. 3(a) and
281 RCP8.5 (Fig. 3(b)), pH reductions crossing the -0.2 threshold are projected for continental
282 slopes and a latitudinal band extending from 55°N to 65°N. Since the pH perturbation
283 originates at the sea-surface, the continental slope and topographic heights (e.g. mid-Atlantic
284 ridge) experience the largest pH reductions. Increasing impact on the sea floor between
285 RCP4.5 and RCP8.5 for a threshold of -0.2 reflects the depth exposure to the pH perturbation
286 of continental slopes and the mid-Atlantic ridge. In summary, the spatial pattern is set by a
287 combination of topography and North Atlantic circulation pathways. It reflectsthe transfer of

288 the surface born anomaly of pH to the ocean interior during deep water formation and
289 downstream transport away from convection sites by the deep western boundary current.

290

291 By the end of the twenty-first century, projected pH reductions (Table 1) cross the -0.2
292 threshold for all scenarios, but RCP2.6. For RCP2.6, deep-water pH reductions remain below
293 thresholds with likely limited impact on benthic environments. Under moderate RCP4.5, a
294 decrease in pH beyond -0.2 units is projected for large areas of the North Atlantic with about
295 $16.7 \pm 4.2\%$ of the sea floor area below 500 m being impacted. This estimate increases to
296 $21.0 \pm 4.4\%$ of the North Atlantic sea floor area under the most severe scenario (RCP8.5) and
297 is still $14.0 \pm 3.3\%$ of the sea floor for a threshold of -0.3. The area impacted does not scale
298 linearly with atmospheric CO₂ (Table 1), but levels off at higher RCPs for threshold -0.2. The
299 -0.3 pH unit threshold (a 100% increase of [H⁺]) is not reached for RCP4.5 and only modest
300 impacts are projected for RCP6.0 (Table 1). We expect, however, an increase in impacted
301 area for all scenarios and pH thresholds beyond 2100 in response to legacy effects of CO₂
302 emissions and ongoing downward propagation of the pH perturbation (Frölicher and Joos,
303 2010).

304

305 3.2.1 Opposing effects of climate change and ocean acidification

306

307 The progression from RCP2.6 to RCP8.5 corresponds to a series of increasing geochemical
308 (atmospheric pCO₂) and physical (climate change, defined here as changes in ocean dynamics
309 in response to atmospheric warming) forcing with opposing effects on deep ocean
310 acidification.

311 In order to distinguish between the physical and geochemical drivers of North Atlantic deep-
312 water acidification, we assessed two contrasting simulations available for two Earth system
313 models (GFDL-ESM2M and IPSL-CM5A-LR) for RCP4.5. The first simulation (Fig. 4 (a))
314 includes climate change effects on ocean circulation and geochemical effects on the seawater
315 CO₂ system in response to atmospheric pCO₂ increase (RCP4.5). In the second experiment
316 (Fig. 4(b)), the circulation and ocean physics are kept at pre-industrial conditions, but
317 atmospheric CO₂ levels following RCP4.5 are used to force ocean acidification
318 (RCP4.5/fixclim). The difference in pH between RCP4.5 and RCP4.5/fixclim (Fig. 4(c))

319 allows, at first order and within the limits of non-linearities (Schwinger et al., 2014), isolation
320 of the effect of climate change on pH changes. The negative differences in pH on panel (c)
321 indicate stronger acidification in RCP4.5/fixclim, and suggest a slight alleviation of ocean
322 acidification at depth and over the time-scale of this study by climate-change. In the
323 experiment where ocean circulation was held at pre-industrial condition (RCP4.5/fixclim)
324 there was a small increase in the area impacted by pH reductions for all thresholds (Table 1).
325 Largest differences in projected pH values between RCP4.5/fixclim and RCP4.5 co-occur
326 with large negative anomalies in winter mixed layer depth maxima in the Labrador Sea and
327 negative pH anomalies downstream of convection sites following the deep western boundary
328 current (Doney and Jenkins, 1994). This is in line with the projected enhancement of
329 stratification across the North Atlantic in response to increasing temperatures and freshening.
330 It will result in changes in winter mixed layer depth, deep convection and a decrease in the
331 Atlantic Meridional Overturning Circulation (Mehl et al., 2007; Cheng et al., 2013). While
332 increasing atmospheric CO₂ reduces pH, increasing climate change reduces surface-to-deep
333 water exchange. In addition, topography modulates the extent of deep-water acidification. The
334 combination of climate-change, the non-linearities of the carbonate system and topography
335 explains the levelling-off of impacts in Table 1 for pH reductions exceeding -0.2.

336 3.2.2 Projected impacts on ecosystems

337

338 In order to evaluate the risk for specific benthic ecosystems to be affected by pH reductions,
339 we co-located seamounts (Figure 3, black dots) and deep-sea canyons (Figure 3, red dots) -
340 both of which are key habitats of high biodiversity - and pH changes for RCP4.5 and RCP8.5
341 separately computed from the multi-model mean (see supplementary material for RCP2.6 and
342 RCP6.0). To further the evaluation of potential impacts of pH reductions beyond pH
343 thresholds, we computed the area of seamounts for which a corresponding decrease is
344 projected. A significant proportion of these habitats will be impacted by pH reductions
345 exceeding -0.2 units by the end of the 21st century under moderate to high emission scenarios
346 (Fig. 5). The geographic pattern results in close to 22.5±5.3% (14.7±4.1%) of North Atlantic
347 deep-sea canyons and 7.7±3.6% (2.7±0.9%) of seamount ecosystems being exposed to pH
348 reductions exceeding -0.2 (-0.3) units under RCP8.5. Under the moderate scenario, RCP4.5,
349 model projections indicate that 21.8±6.0% of deep-sea canyons and 5.0±1.6% of seamounts
350 still will experience pH reductions exceeding the -0.2 threshold. The close to constant impact

351 reflects the use of a diagnostic that is based on counts of features being impacted, in addition
352 to the depth distribution and propagation of the pH anomaly.

353

354 Seamounts and deep-sea canyons are known as hotspots of biodiversity and harbour a variety
355 of distinct communities including reef-building cold-water corals, soft coral gardens and
356 deep-sea sponge aggregations (Buhl-Mortensen et al., 2010, 2012; Clark et al., 2010; De Leo
357 et al., 2010; ICES, 2007). Recent assessments reveal a high level of anthropogenic pressures
358 on these ecosystems (Clark et al., 2010, Ramirez-Llodra et al., 2011). While fishing and
359 resource extraction are recognized as the dominant human pressures at present and in the near
360 future, expert assessments highlight the need for an appropriate quantification of the impacts
361 of climate change and ocean acidification (Taranto et al., 2012). Present international
362 conservation targets aim at preserving 10% of marine biomes by 2020 (CBD, 2011).
363 Although not directly comparable to the outcome of model projections, it is nevertheless of
364 interest to confront this preservation target with model results suggesting that ~ 8% of North
365 Atlantic seamounts and 23% of canyons will experience a decrease in pH exceeding 0.2 pH
366 units by the year 2100 for the most severe scenario. Seamounts identified as marine protection
367 areas in the OSPAR region and excluding active venting sites (e.g. Josephine seamount,
368 36°40.02'N 14°15.00'W; Sedlo seamount, 40°12.8'N 26°15.8'W) fall within the area for which
369 these pH reductions are projected.

370

371 Our knowledge of the ecology of deep benthic communities is still limited and impacts of pH
372 changes on these communities are difficult to evaluate owing to lack of experimental and
373 observational data. Rapid changes in pH will likely lead to disruption of extracellular acid-
374 base balance, impedance of calcification and other physiological effects in deep-water
375 organisms, and whatever acclimation is required may have increased energetic costs
376 (Widdicombe and Spicer, 2008) – e.g. for metabolism/maintenance, growth, reproduction –
377 and could extend to increases in mortality of both adults and juveniles. Changes at the
378 individual and population level will inevitably lead to more widespread ecosystem and
379 community level changes and potential shifts in biodiversity (Hendriks et al., 2010) and
380 ecosystem functioning (Danovaro et al., 2008). Biodiversity reductions could arise from a loss
381 of species, functional, or even taxonomic groups sensitive to pH change. The ecological
382 implications of pH change could be more severe if keystone or habitat-forming species are

383 impacted (Widdicombe and Spicer, 2008), which seems likely (Guinotte et al., 2006). These
384 effects may be likely exacerbated in the presence of other stressors (Walther et al., 2009), such
385 as global warming and projected reductions in deep-sea food supply (Bopp et al., 2013), as
386 well as elevated resource exploitation and pollution. In particular, reductions in food supply to
387 deep benthic communities are projected to result in a decrease in biomass and a shift towards
388 smaller sized organisms (Jones et al., 2013). These changes will modify energy transfer rates
389 through benthic food webs and may leave communities more susceptible to pH reductions.
390 We propose these and future model projections to be taken into account when defining long-
391 term preservation and management approaches to deep-sea ecosystems.

392

393 **4 Conclusions**

394 This study assesses the potential for detrimental pH reduction to occur across the deep North
395 Atlantic by the end of the 21st century. It evaluates results from seven fully-coupled Earth
396 system models and for four representative concentration pathways ranging from RCP2.6 to
397 RCP8.5. In three out of the four scenarios, the multi-model analysis suggests that by 2100
398 over 17% of the seafloor area below 500m depth in the North Atlantic sector will experience
399 pH reductions exceeding -0.2 units. Enhanced stratification in response to warming and
400 freshening of surface waters slightly counteracts deep-water acidification. pH reductions co-
401 occur with sites of high deep-sea biodiversity such as seamounts and canyons. Model
402 projections indicate that by the end of this century and for the high CO₂ scenario RCP8.5,
403 close to 23% (~15%) of North Atlantic deep-sea canyons and ~8% (3%) of seamounts will
404 experience pH reductions exceeding -0.2 (-0.3) units. Seamounts proposed as sites of marine
405 protected areas are concerned by these pH reductions. The spatial pattern of impacts reflects
406 the depth of the pH perturbation and did not scale linearly with atmospheric CO₂
407 concentration. Impacts may cause negative changes of the same magnitude or exceeding the
408 current biodiversity target of 10% of preservation of marine biomes implying that ocean
409 acidification may offset benefits from conservation/management strategies relying on the
410 regulation of resource exploitation.

411

412 **Acknowledgements**

413 This work was supported through EU FP7 projects EPOCA (grant no. 211384) and
414 CARBOCHANGE (grant no. 264879). DJ was funded by the UK Natural Environment
415 Research Council as part of the Marine Environmental Mapping Programme (MAREMAP).
416 SCD acknowledges support from the National Science Foundation (AGS-1048827). FJ
417 acknowledges support from the Swiss National Science Foundation. This is a contribution
418 from the BIOFEEDBACK project of the Centre for Climate Dynamics at Bjerknes Centre. C.
419 Heinze and J. Tjiputra are grateful for support through NOTUR projects NN2980K and
420 NN2345K as well as NorStore projects NS2980K and NS2345K for HPC CPU time and data
421 storage. To analyze the CMIP5 data, this study benefited from the IPSL Prodiguer-Ciclad
422 facility which is supported by CNRS, UPMC, Labex L-IPSL which is funded by the ANR
423 (Grant #ANR-10-LABX-0018) and by the European FP7 IS-ENES2 project (Grant #312979).

424 **References**

- 425 Barry, J. P., Buck, K. R., Lovera, C., Kuhnz, L. and Whaling, P. J.: Utility of deep sea CO₂
426 release experiments in understanding the biology of a high-CO₂ ocean: Effects of hypercapnia
427 on deep sea meiofauna. *J. Geophys. Res.*, 110, C09S12, doi:10.1029/2004JC002629, 2005.
- 428 Barry, J. P., Widdicombe, S. and Hall-Spencer, J. M.: Effects of ocean acidification on marine
429 biodiversity and ecosystem function. *Ocean Acidification*, eds Gattuso, J.-P., Hansson, L.,
430 Oxford University Press, pp. 192-209, 2011.
- 431 Barry, J. P., Buck, K. R., Lovera, C., Brewer, P. G., Seibel, B. A., Drazen, J. C., Tamburri, M.
432 N., Whaling, P. J., Kuhnz, L., Pane, E. F.: The response of abyssal organisms to low pH
433 conditions during a series of CO₂-release experiments simulating deep-sea carbon
434 sequestration. *Deep Sea Research Part II: Topical Studies in Oceanography* 92 (0), 249-260,
435 2013.
- 436 Billé, R., Kelly, R., Biastoch, A., Harrould-Kolieb, E., Herr, D., Joos, F., Kroeker, K.,
437 Laffoley, D., Oschlies, A., Gattuso, J.-P.: Taking action against ocean acidification: A review
438 of management and policy options, *Environmental Management*, 52/4, 761-779, 2013.
- 439 Bopp, L., Resplandy, L., Orr, J. C., Doney, S. C., Dunne, J. P., Gehlen, M., Halloran, P.,
440 Heinze, C., Ilyina, T., Séférian, R., Tjiputra, J., and Vichi, M.: Multiple stressors of ocean
441 ecosystems in the 21st century: projections with CMIP5 models, *Biogeosciences*, 10, 6225-
442 6245, doi:10.5194/bg-10-6225-2013, 2013.
- 443 Bryan, F.: High-latitude salinity effects and interhemispheric thermohaline circulations, *Nature*,
444 323, 301–304, 1986.
- 445 Buhl-Mortensen, L., Vanreusel, A., Gooday, A. J., Levin, L. A., Priede, I. G., Buhl-Mortensen,
446 P., Gheerardyn, H., King, N.J., and Raes, M.: Biological structures as a source of habitat
447 heterogeneity and biodiversity on the deep ocean margins. *Marine Ecology* 31(1): 21-50,
448 2010.
- 449 Buhl-Mortensen, L., Buhl-Mortensen, P., Dolan, M. F. J., Dannheim, J., Bellec, V., and Holte,
450 B. 2012. Habitat complexity and bottom fauna composition at different scales on the
451 continental shelf and slope of northern Norway. *Hydrobiologia*, 685:191-219: 2012.

452 Cheng, W., Chiang, J., and Zhang, D.: Atlantic Meridional Overturning Circulation (AMOC) in
453 CMIP5 models: RCP and Historical Simulations, *J. Climate*, 26, 7187–7197,
454 doi:10.1175/JCLI-D-12-00496.1, 2013.

455 Childress, J. J.: Are there physiological and biochemical adaptations of metabolism in deep-sea
456 animals, *Trends in Ecology and Evolution*, 10, 1–36, 1995.

457 Clark, M. R., Rowden, A. A., Schlacher, T., Williams, A., Consalvey, M., Stocks, K. I.,
458 Rogers, A. D., O'Hara, T. D., White, M., Shank, T. M. and Hall-Spencer, J. M.: The ecology
459 of seamounts: structure, function, and human impacts, *Annu. Rev. Mar. Sci.* 2, 253–278,
460 doi:10.1146/annurev-marine-120308-081109, 2010.

461 Clauss, G., and Hoog, S.: Deep Sea Challenges of Marine Technology and Oceanographic
462 Engineering,
463 Developments in Marine Technology 12, Science-Technology Synergy for Research in the
464 Marine Environment: Challenges for the XXI Century, Elsevier, Oxford, England, 2002.

465 Convention on Biodiversity (CBD), target 11, document COP/10/INF/12/Rev.1,
466 <http://www.cbd.int/sp/targets/rationale/target-11/>.

467 Danovaro, R., Gambi, C., Dell'Anno, A., Corinaldesi, C., Fraschetti, S., Vanreusel, A., Vincx,
468 M. and Gooday, A. J.: Exponential decline of deep-sea ecosystem functioning linked to
469 benthic biodiversity loss, *Curr. Biol.*, 18, 1-8, 2008.

470 De Leo, F. C., Smith, C. R., Rowden, A. A., Bowden, D. A. and Clark, M. R.: Submarine
471 canyons: hotspots of benthic biomass and productivity in the deep sea, *Proc. R. Soc. B.*, 277,
472 2783-2792 doi:10.1098/rspb.2010.0462, 2010.

473 Doney, S. C. and Jenkins, W. J.: Ventilation of the deep western boundary current and the
474 abyssal western North Atlantic: estimates from tritium and ³He distributions, *J. Phys.*
475 *Oceanogr.*, 24, 638-659, 1994.

476 Duarte, C. M., Hendriks, I. E., Moore, T.S., Olsen, Y. S., Steckbauer, A., Ramajo, L.,
477 Carstensen, J., Trotter J. A., McCulloch, M.: Is Ocean Acidification an Open-Ocean
478 Syndrome? Understanding Anthropogenic Impacts on Seawater pH, *Estuaries and Coasts*, 36,
479 221-236, doi:10.1007/s12237-013-9594-3, 2013.

480 Elderfield, H., Ferretti, P., Greaves, M., Crowhurst, S., McCave, I. N., Hodell, D. and
481 Piotrowski, A.M.: Evolution of Ocean Temperature and Ice Volume Through the Mid-
482 Pleistocene Climate Transition, *Science*, 337, 704-709, doi:10.1126/science.1221294, 2012.

483 Fautin, D. G., Guinotte, J. M., Orr, J. C.: Comparative depth distribution of corallimorpharians
484 and scleractinians (Cnidaria: Anthozoa), *Mar. Ecol. Prog. Ser.*, 397, 63–70, 2009.

485 Fleeger, J. W., Carman, K. R., Weisenhorn, P. B., Sofranko, H., Marshall, T., Thistle, D.,
486 Barry, J.P. Simulated sequestration of anthropogenic carbon dioxide at a deep-sea site: Effects
487 on nematode abundance and biovolume. *Deep Sea Research Part I: Oceanographic Research*
488 *Papers* 53 (7), 1135-1147, 2006.

489 Frölicher, T. L. and Joos, F.: Reversible and irreversible impacts of greenhouse gas emissions
490 in multi-century projections with the NCAR global coupled carbon cycle-climate model,
491 *Clim. Dyn.*, 35: 1439-1459, 2010.

492 Gehlen, M., L. Bopp and O. Aumont: The short-term dissolution response of pelagic carbonate
493 sediments to the invasion of anthropogenic CO₂ : A model study, *Geochem. Geophys.*
494 *Geosyst.*, 9 Q02012, doi: 10.1029/2007GC001756, 2008.

495 González-Dávila, M., Santana-Casiano, J. M., Rueda, M. J. and Llinás, O.: The water column
496 distribution of carbonate system variables at the ESTOC site from 1995 to 2004,
497 *Biogeosciences*, 7, 3067-3081, 2010.

498 Guinotte, J. M., Orr, J., Cairns, S., Freiwald, A., Morgan, L. and George, R.: Will human-
499 induced changes in seawater chemistry alter the distribution of deep-sea scleractinian corals?
500 *Front. Ecol. Environ.*, 4, 141–146, 2006.

501 Harris, P. T. and Whiteway, T.: Global distribution of large submarine canyons: Geomorphic
502 differences between active and passive continental margins, *Mar. Geol.*, 285, 69-86, 2011.

503 Hendriks, I. E., Duarte, C. M. and Álvarez, M.: Vulnerability of marine biodiversity to ocean
504 acidification: A meta-analysis, *Est., Coast. and Shelf Sci.*, 86, 157-164, 2010.

505 Hofmann, G. E., Smith, J. E., Johnson, K. S., Send, U., Levin, L. A., Micheli, F., Paytan, A.,
506 Price, N. N., Peterson, B., Takeshita, Y., Matson, P. G., Crook, E. D., Kroeker, K. J., Gambi,
507 M. C., Rivest, E. B., Frieder, C. A., Yu, P. C., Martz, T. R.: High-Frequency Dynamics of
508 Ocean pH: A Multi-Ecosystem Comparison, *PLoS ONE*, 6(12), e28983.
509 doi:10.1371/journal.pone.0028983, 2011.

510 Hönisch, B., Ridgwell, A., Schmidt, D. N., Thomas, E., Gibbs, S. J., Sluijs, A., Zeebe, R.,
511 Kump, L., Martindale, R. C., Greene, S. E., Kiessling, W., Ries, J., Zachos, J. C., Royer, D.
512 L., Barker, S., Marchitto, T. M., Moyer, R., Pelejero, C., Ziveri, P., Foster, G. L. and
513 Williams, B.: The Geological Record of Ocean Acidification, *Science*, 335, 1058-1063, 2008.

514 ICES, Report of the Working Group on Deep-water Ecology 26-28, ICES CM 2007/ACE:01
515 Ref. LRC, International Council for the Exploration of the Sea, Copenhagen, Denmark, 61
516 pp., 2007.

517 IPCC (2011) Workshop Report of the Intergovernmental Panel on Climate Change Workshop
518 on Impacts of Ocean Acidification on Marine Biology and Ecosystems, eds Field CB et al.
519 (IPCC Working Group II Technical Support Unit, Carnegie Institution, Stanford, California,
520 United States of America), pp. 164.

521 Jones, D. O. B., Yool, A., Wei, C.-L., Henson, S. A., Ruhl, H. A., Watson, R. A. and Gehlen,
522 M.: Global reductions in seafloor biomass in response to climate change, *Global Change*
523 *Biology*, 20(6), 1864-1873, doi: 10.1111/gcb.12480, 2014.

524 Khatiwala, S., Tanhua, T., Mikaloff-Fletcher, S., Gerber, M., Doney, S. C., Graven, H. D.,
525 Gruber, N., McKinley, G. A., Murata, A., Ríos, A. F., and Sabine, C. L.: Global ocean storage
526 of anthropogenic carbon, *Biogeosciences*, 10, 2169-2191, doi:10.5194/bg-10-2169-2013,
527 2013.

528 Kroeker, K.J., Kordas, R. L., Crim, R. N. and Singh, G. G.: Meta-analysis reveals negative yet
529 variable effects of ocean acidification on marine organisms, *Ecology Letters*, 13, 1419-1434,
530 2010.

531 Marchal, O., Stocker, T. F., Joos, F., Indermühle, A., Blunier, T. and Tschumi, J: Modeling the
532 concentration of atmospheric CO₂ during the Younger Dryas climate event, *Clim. Dynam.*, 15,
533 341–354, 1999.

534 Matsumoto, K. and Yokoyama, Y.: Atmospheric $\Delta^{14}C$ reduction in simulations of Atlantic
535 overturning circulation shutdown, *Global Biogeochem. Cycles* 27: 296–304,
536 doi:10.1002/gbc.20035, 2013.

537 Meehl, G.A., Stocker, T. F., Collins, W. D., Friedlingstein, P., Gaye, A. T., Gregory, J. M.,
538 Kitoh, A., Knutti, R., Murphy, J. M., Noda, A., Raper, S. C. B., Watterson, I. G., Weaver, A.
539 J. and Zhao, Z.-C.: Global Climate Projections. In: *Climate Change 2007: The Physical*
540 *Science Basis*. Contribution of Working Group I to the Fourth Assessment Report of the

541 Intergovernmental Panel on Climate Change [Solomon, S., D. Qin, M. Manning, Z. Chen, M.
542 Marquis, K.B. Averyt, M. Tignor and H.L. Miller (eds.)]. Cambridge University Press,
543 Cambridge, United Kingdom and New York, NY, USA, 2007.

544 Moss, R. H., Edmonds, J. A., Hibbard, K. A., Manning, M. R., Rose, S. K., van Vuuren, D. P.,
545 Carter, T. R., Emori, S., Kainuma, M., Kram, T., Meehl, G. A., Mitchell, J. F. B.,
546 Nakicenovic, N., Riahi, K., Smith, S. J., Stouffer, R. J., Thomson, A. M., Weyant, J. P. and
547 Wilbanks, T. J.: The next generation of scenarios for climate change research and assessment,
548 *Nature*, 463, 747-756, 2010.

549 Orr, J. C., Fabry, V. J., Aumont, O., Bopp, L., Doney, S. C., Feely, R. A., Gnanadesikan, A.,
550 Gruber, N., Ishida, A., Joos, F., Key, R. M., Lindsay, K., Maier-Reimer, E., Matear, R.,
551 Monfray, P., Mouchet, A., Najjar, R. G., Plattner, G.-K., Rodgers, K. B., Sabine, C. L.,
552 Sarmiento, J. L., Schlitzer, R., Slater, R. D., Totterdell, I. J., Weirig, M.-F., Yamanaka, Y. and
553 Yool, A.: Anthropogenic ocean acidification over the twenty-first century and its impact on
554 calcifying organisms, *Nature*, 437, 681-686, 2005.

555 Orr, J. C.: Recent and future changes in ocean carbonate chemistry.
556 *Ocean Acidification*. J.-P. Gattuso and L. Hansson (Eds.), Oxford University Press, Oxford,
557 41-66, 2011.

558 Ramirez Llodra, E.: Fecundity and life-history strategies in marine invertebrates, *Advances in*
559 *Marine Biology*, 43, 87-170, 2002.

560 Ramirez-Llodra, E., Tyler, P. A., Baker, M. C., Bergstad, O. A., Clark, M. R., Escobar, E.,
561 Levin, L. A., Menot, L., Rowden, A. A., Smith, C. R. and Van Dover, C. Ø.: Man and the
562 Last Great Wilderness: Human Impact on the Deep Sea, *PLoS ONE*, 6(8), e22588,
563 doi:10.1371/journal.pone.0022588, 2011.

564 Roth, R. and Joos, F.: A reconstruction of radiocarbon production and total solar irradiance
565 from the Holocene ¹⁴C and CO₂ records: implications of data and model uncertainties, *Climate*
566 *of the Past*, 9, 1879-1909, 2013.

567 Sabine, C. L., Feely, R. A., Gruber, N., Key, R. M., Lee, K., Bullister, J. L., Wanninkhof, R.,
568 Wong, C. S., Wallace, D. W. R., Tilbrook, B., Millero, F. J., Peng, T.-H., Kozyr, A., Ono, T.
569 and Rios, A. F.: The oceanic sink for anthropogenic CO₂, *Science*, 305, 367–371, 2004.

570 Sanyal, A., Hemming, N. G., Hanson, G. N. and Broecker, W. S.: Evidence for a higher pH in
571 the glacial ocean from boron isotopes in foraminifera, *Nature*, 373, 234-236, 1995.

572 Schubert, R., Schellnhuber, H.-J., Buchmann, N., Epiney, A., Griesshammer, R., Kulesa, M.,
573 Messner, D., Rahmstorf, S., Schmid, J. : The future oceans - Warming up, rising high, turning
574 sour, Special Report by the German Advisory Council on Global Change (WBGU), 123 pp.,
575 2006.

576 Schwinger, J., Tjiputra, J. F., Heinze, C., Bopp, L., Christian, J. R., Gehlen, M., Ilyina, T.,
577 Jones, C. D., Salas-Méla, D., Segschneider, J., Séférian, R., and Totterdell, I.: Non-linearity
578 of ocean carbon cycle feedbacks in CMIP5 earth system models, *J. Climate*, 27(11), 3869-
579 3888. [doi:10.1175/JCLI-D-13-00452.1](https://doi.org/10.1175/JCLI-D-13-00452.1), 2014.

580 Seibel, B. A. And Walsh, P. J. Potential Impacts of CO₂ Injection on Deep-Sea Biota, *Science*
581 294, 319, 2001.

582 Seibel, B. A. and Walsh, P. J.: Biological impacts of deep-sea carbon dioxide injection inferred
583 from indices of physiological performance, *Journal of Experimental Biology*, 206, 641-650,
584 2003.

585 Somero, G. N.: The Physiology of Global Change: Linking Patterns to Mechanisms, *Annu.*
586 *Rev. Mar. Sci.*, 4, 39-61, 2012.

587 Steinacher, M., Joos, F. and Stocker, T. F.: Allowable carbon emissions lowered by multiple
588 climate targets, *Nature*, 499, 197-201, 2013.

589 Taranto, G. H., Kvile, K. Ø., Pitcher, T. J. and Morato, T.: An Ecosystem Evaluation
590 Framework for Global Seamount Conservation and Management. *PLoS ONE*, 7, e42950,
591 [doi:10.1371/journal.pone.0042950](https://doi.org/10.1371/journal.pone.0042950), 2012.

592 Taylor, K. E., Stouffer, R. J. and Meehl, G. A.: An overview of CMIP5 and the experiment
593 design, *Bull. Am. Meteor. Soc.*, 93, 485–498, [doi:10.1175/ BAMS-D-11-00094](https://doi.org/10.1175/BAMS-D-11-00094), 2011.

594 Tittensor, D. P., Baco A. R., Hall-Spencer, J. M., Orr, J. C. and Rogers, A. D., Seamounts as
595 refugia from ocean acidification for coldwater stony corals, *Marine Ecology*, 31, 212–225,
596 2010.

597 Van Vuuren, D. P., Edmonds, J., Kainuma, M., Riahi, K., Thomson, A., Hibbard, K., Hurtt, G.
598 C., Kram, T., Krey, V., Lamarque, J. -F., Masui, T., Meinshausen, M., Nakicenovic, N.,
599 Smith, S. J. and Rose, S. K.: The representative concentration pathways: an overview, *Clim.*
600 *Change.*, 109, 5-31, [doi: 10.1007/s10584-011-0148-z](https://doi.org/10.1007/s10584-011-0148-z), 2011.

- 601 Walther, K., Sartoris, F. J., Bock, C. and Pörtner, H. O.: Impact of anthropogenic ocean
602 acidification on thermal tolerance of the spider crab *Hyas araneus*, *Biogeosciences*, 6, 2207-
603 2215, 2009.
- 604 Widdicombe, S. and Spicer, J. I.: Predicting the impact of ocean acidification on benthic
605 biodiversity: What can physiology tell us?, *J. Exp. Mar. Biol. Ecol.*, 366, 187-197, 2008.
- 606 Yesson, C., Clark, M. R., Taylor, M. L. and Rogers, A. D.: The global distribution of
607 seamounts based on 30 arc seconds bathymetry data, *Deep-Sea Res. I*, 58, 442-453,
608 doi:10.1016/j.dsr.2011.02.004, 2011.
- 609 Yu, J., Broecker, W. S., Elderfield, H., Jin, Z., McManus, J. and Zhang, F.: Loss of Carbon
610 from the Deep Sea Since the Last Glacial Maximum, *Science*, 330, 1084-1087, doi:
611 10.1126/science.1193221, 2010.
- 612 Yu, J., Anderson, R. F., Jin, Z., Rae, J. W. B., Opdyke, N. and Eggins, S. M.: Responses of the
613 deep ocean carbonate system to carbon reorganization during the Last Glacial–interglacial
614 cycle, *Quaternary Science Reviews*, 76, 39-52, 2013.

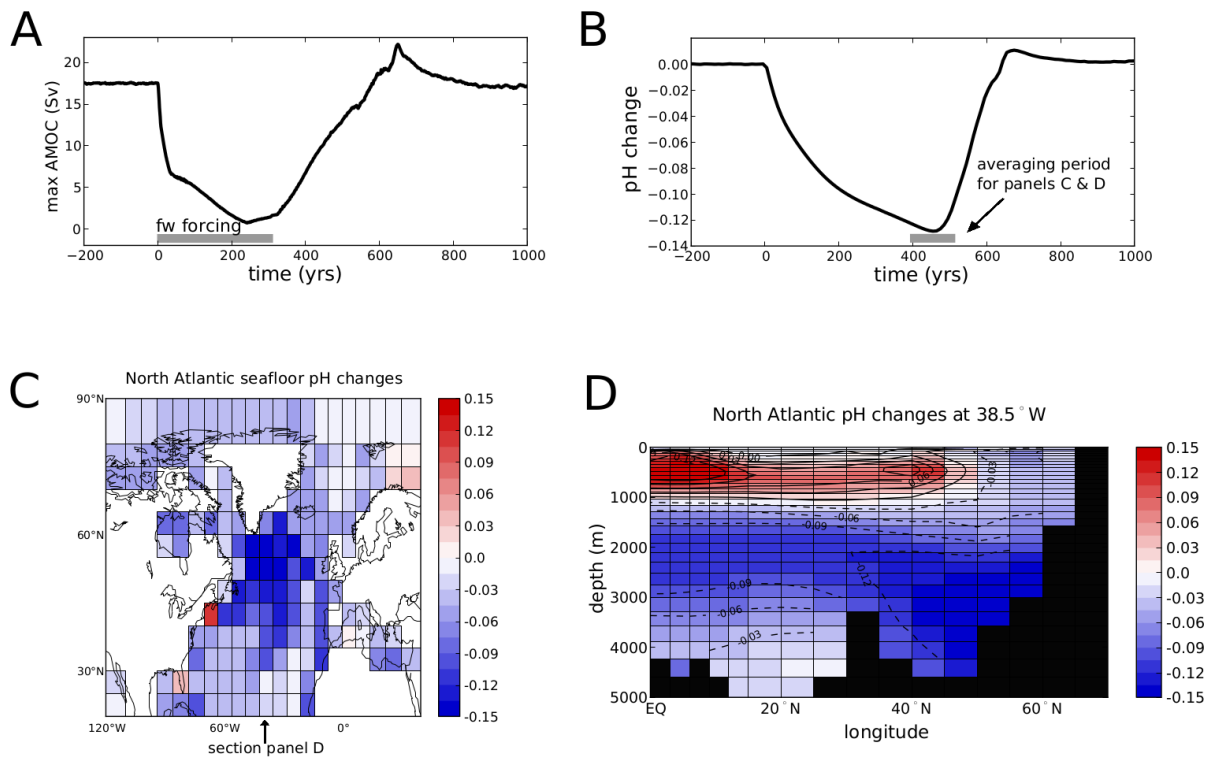
615 Table 1. Fraction of North Atlantic seafloor (35°N-75°N, 90°W-180°W) below 500 m
 616 experiencing a reduction in pH ≥ 0.2 , respectively ≥ 0.3 at the end of the 21st century.
 617 Fractions for multi-model mean and standard deviation are given in percentage of impacted
 618 surface area relative to the total surface seafloor area of the North Atlantic sector. n=number
 619 of simulations available at time of analysis for each RCP

620

	n	pH reduction ≥ 0.2		pH reduction ≥ 0.3	
		mean (%)	std (%)	mean (%)	std (%)
RCP2.6	6	1.2	1.1	0.0	0.1
RCP4.5	7	16.7	4.2	0.6	0.5
RCP4.5/fixclim	2	18.1	n.a	0.8	n.a
RCP6.0	4	19.9	5.0	4.4	1.5
RCP8.5	7	21.0	4.4	14.0	3.3

621

622

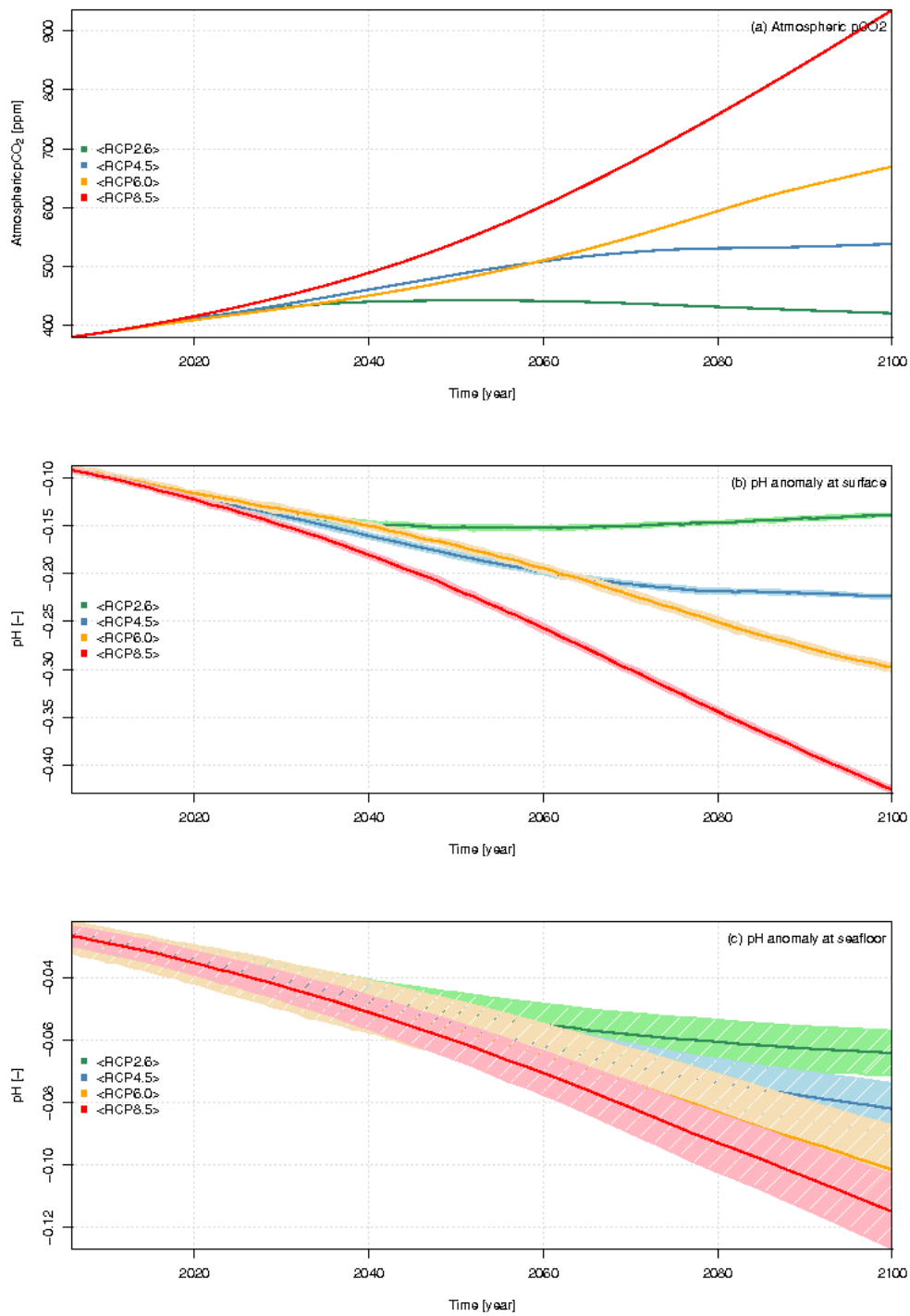


624

625 Figure 1. North Atlantic freshwater hosing experiment. (a) Time series of strength of Atlantic
 626 Meridional Overturning Circulation (Sv), freshwater release occurred over 300 years (grey
 627 bar); (b) times series of pH change relative to pre-industrial averaged over the deep (below
 628 2000 m) Northern Atlantic (45° N – 65° N); (c) spatial distribution of the pH-reduction
 629 averaged over experiment years 400-450 (grey bar on panel (b)) in terms of pH anomalies
 630 relative to pre-industrial at the seafloor and (d) in a section through the Atlantic at 38.5° W.

631

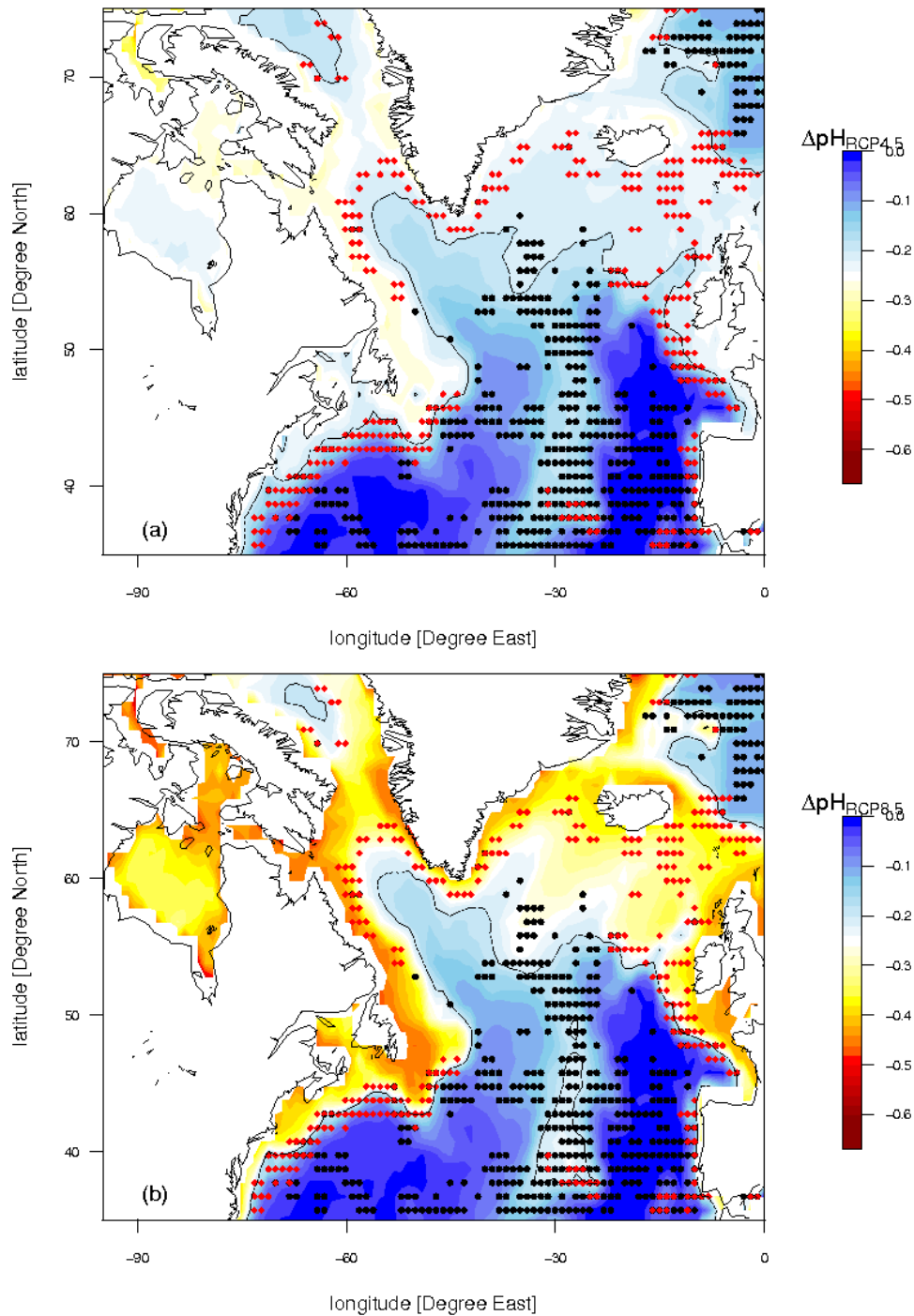
632



633

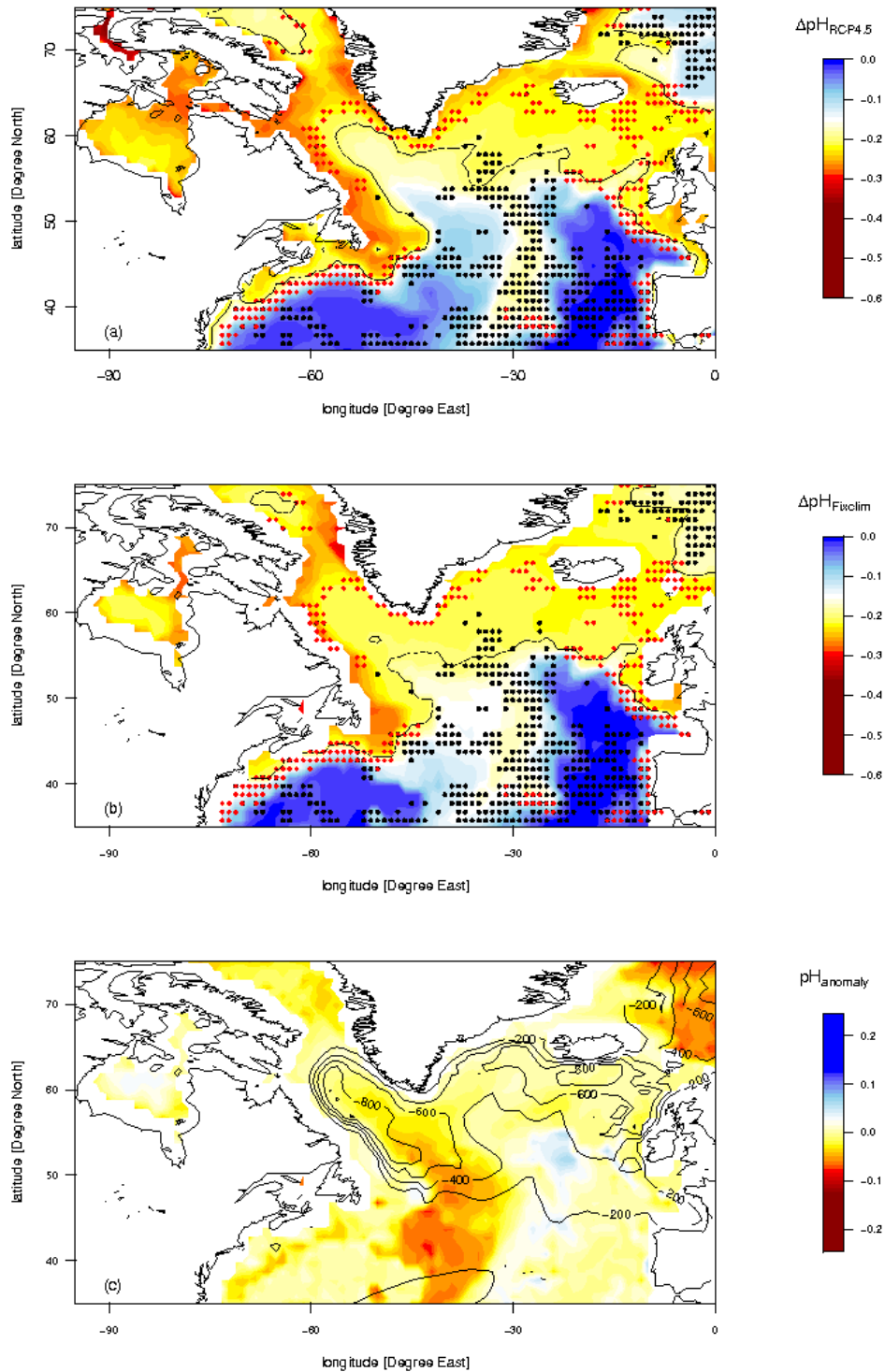
634 Figure 2. Time-series of (a) atmospheric CO₂ (ppm) for RCP2.6, RCP4.5, RCP6.0 and
 635 RCP8.5 scenarios between 2006 and 2100 and corresponding simulated average North
 636 Atlantic pH changes relative to the pre-industrial mean for (b) surface waters and (c) deep
 637 waters. Hatching indicates the 2.5%-97.5% confidence interval of multi-model averages.

638



639

640 Figure 3. Projected changes in pH between pre-industrial and the experiments forced by IPCC
 641 RCP scenarios by 2100. The panels show ensemble-mean differences in pH between the pre-
 642 industrial and the 2090-2100 average for (a) RCP4.5 and (b) RCP8.5. Locations of deep-sea
 643 canyons and seamounts are indicated as red and black symbols, respectively. The -0.2 pH
 644 contour line is plotted to delineate areas experiencing pH reductions beyond this threshold.

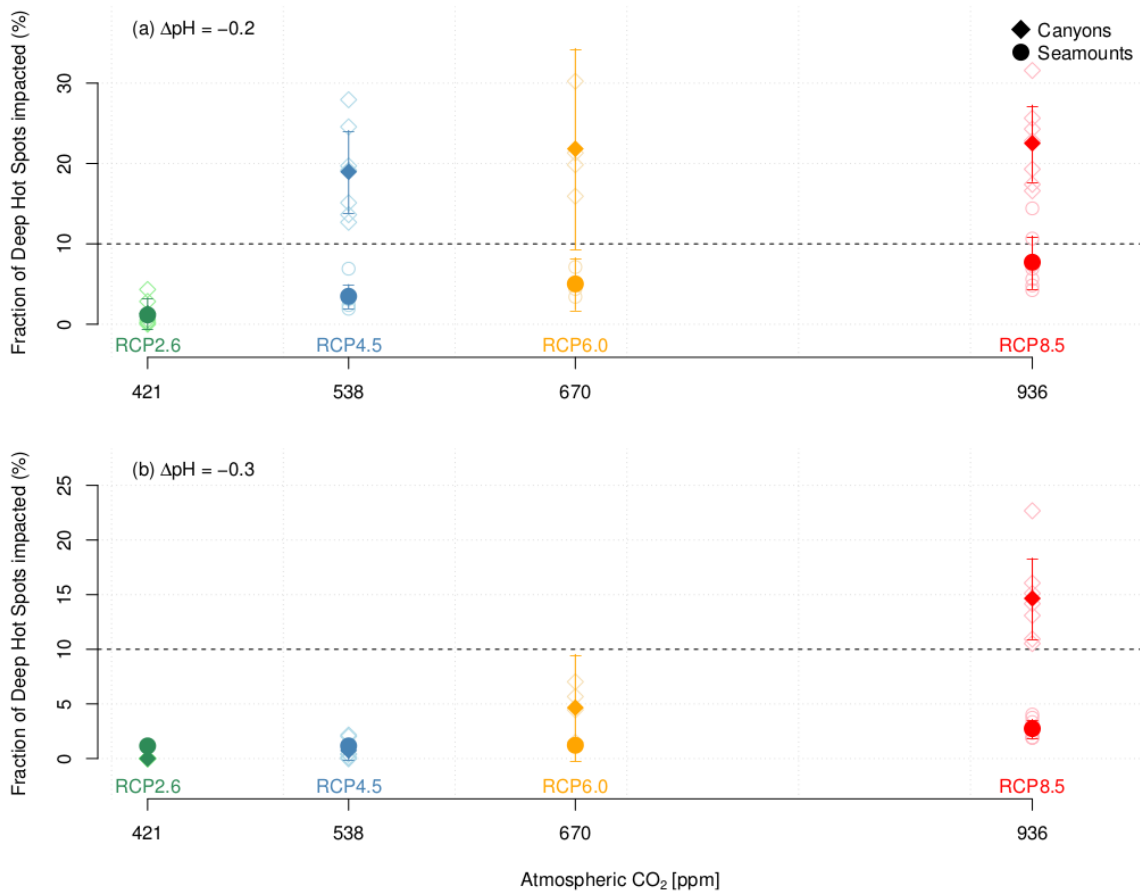


646 Figure 4. Projected changes in deep ocean pH between pre-industrial and experiments forced
 647 with RCP scenarios by 2100: (a) RCP4.5, (b) RCP4.5/fixclim, (c) difference in pH between
 648 (a) and (b) together with changes in maximum winter mixed layer depth (contour lines). The

649 change in pH is computed as the difference in mean pH between the pre-industrial and the
650 2090-2100 average.

651

652



654 Figure 5. Projected impacts on seamounts (circles) and canyons (diamonds) as a function of
655 atmospheric CO₂ levels by year 2100 for pH reductions exceeding (a) -0.2 and (b) -0.3.
656 Impact is computed as the fraction of the surface area affected by a reduction exceeding the
657 threshold for seamounts, respectively as the number of canyons surrounded by waters for
658 which the reduction in pH exceeding the threshold is projected. Model pH is the decadal mean
659 (2090-2100). Note that the seamount and canyon multi-model averages for the RCP2.6
660 scenario overlay each other. Light coloured circles: values obtained for each Earth system
661 model; dark coloured circles: multi-model average for each scenario. Vertical and horizontal
662 bars: 2.5%-97.5% confidence interval of multi-model averages.